

X-ray, multispectral and chlorophyll fluorescence images: innovative methods for evaluating the physiological potential of rice seeds

Artur Sousa Silva^{1*}, Silvio Moure Cicero¹, Fabiano França da Silva¹,
Francisco Guilhien Gomes-Junior¹

ABSTRACT: Image analysis techniques are expanding in agriculture and, for being fast, simple, and not destroying samples, they are interesting alternatives in the detection of immature rice seeds. Therefore, the aim of this study was to evaluate the quality of rice seeds using X-ray, multispectral and chlorophyll fluorescence image analysis techniques. Initially, with the seeds identified and numbered, radiographic images were obtained to determine the free space (area between the endosperm + embryo and the glumes). Subsequently, with the same seeds used in the X-ray, multispectral and chlorophyll fluorescence images were acquired, and then the computerized seedling analysis was performed with the SVIS[®] software. It was concluded that rice seeds that do not germinate or originate abnormal seedlings have free space equal to or greater than 18.68%, higher reflectance in the spectral bands with wavelength from 590 nm to 780 nm (41.46% to 64.21%, respectively) and in the band of 970 nm (75.65%), in addition to having chlorophyll fluorescence values equal to or greater than 40.58 and 112.92 at excitation/emission energies of 630/700 nm and 645/700 nm, respectively.

Index terms: free space, immature seeds, *Oryza sativa* L., seed vigor, spectral reflectance.

RESUMO: As técnicas de análise de imagens apresentam-se em expansão na agricultura e por consistirem em avaliações rápidas, simples e não destrutivas, são alternativas interessantes para a detecção de sementes de arroz imaturas. Assim, o objetivo deste trabalho foi avaliar a qualidade de sementes de arroz utilizando as técnicas de análise de imagens de raios X, multiespectrais e de fluorescência de clorofila. Inicialmente, com as sementes identificadas e enumeradas, foram obtidas imagens radiográficas para a obtenção do espaço vazio (área entre o endosperma + embrião e as glumelas). Posteriormente, com as mesmas sementes utilizadas na análise de raios X, procedeu-se a aquisição das imagens multiespectrais e de fluorescência de clorofila. Na sequência, realizou-se a análise computadorizada de plântulas com o software SVIS[®]. Concluiu-se que as sementes de arroz que não germinam ou originam plântulas anormais apresentam espaço vazio interno igual ou superior a 18,68%, maior refletância nas bandas espectrais de comprimento de onda de 590 nm a 780 nm (41,46% a 64,21%, respectivamente) e na banda de 970 nm (75,65%), além de apresentarem valores de fluorescência de clorofila iguais ou superiores a 40,58 e a 112,92, respectivamente nas energias de excitação/emissão de 630/700 nm e de 645/700 nm.

Termos para indexação: espaço vazio, sementes imaturas, *Oryza sativa* L., vigor de sementes, refletância espectral.

Journal of Seed Science, v.45,
e202345003, 2023



<http://dx.doi.org/10.1590/2317-1545v45257617>

*Corresponding author
E-mail: artursilva.agro@gmail.com

Received: 10/23/2021.
Accepted: 10/26/2022.

¹Universidade de São Paulo (USP),
Escola Superior de Agricultura
"Luiz de Queiroz" – 13418-900,
Piracicaba, São Paulo, Brasil.

INTRODUCTION

New technologies whose principles are based on the use of computerized systems have been used to evaluate the internal morphology of seeds in a non-destructive way and to evaluate their vigor, since they generate efficient results, with less subjectivity and greater credibility to the process of analysis and quality control. Non-destructive techniques of seed image analysis, such as computer vision, X-ray and spectral images, are efficient for evaluating seed quality, in addition to being simple and fast (Marcos-Filho et al., 2010; Huang et al., 2015).

One of the main techniques of seed image analysis currently used is X-ray analysis, considered very efficient for studies of internal seed morphology, besides being a non-destructive and unharmed to the seed, which allows the examination of internal parts associated with seed quality, such as the degree of embryonic development, from the free space in the internal cavity of the seed, which is directly associated with its performance (Marcos-Filho et al., 2010).

The multispectral imaging technique combines the computer vision technique and spectroscopy to obtain spatial and spectral information of objects, without the need for pre-treatments, allowing the simultaneous measurement of multiple components involved in seed quality, which allows its use for the evaluation of various seed characteristics, identification and classification of cultivars, differences in physiological quality in different lots, detection of insect damage and yeast infection, in addition to the determination of seed chemical composition and seedling quality, the so-called phenotyping (Huang et al., 2015).

However, the use of this technique by the seed industry requires adjustments, standardization and reduction of costs, without compromising the accuracy of the analysis. For example, the evaluation of seed maturation through multi and hyperspectral imaging techniques has been successfully used to obtain chlorophyll fluorescence (CF) of seeds, being highly relevant for quantifying a component with high interconnection with seed quality, the chlorophyll molecule and its principle consists of exciting this molecule at a specific wavelength. The efficiency of the CF technique to evaluate seed quality has already been proven for cabbage (Jalink et al., 1998; Yadav et al., 2015), soybean (Cicero et al., 2009), wheat (Xing et al., 2010), chicory (Ooms and Destain, 2011) and tomato (Li et al., 2016).

Considering the techniques of image analysis as alternatives for the evaluation of seed quality, the aim of this study was to evaluate the quality of rice seeds using X-ray, multispectral and chlorophyll fluorescence imaging techniques and relate this information to the physiological potential of the seeds.

MATERIAL AND METHODS

The experiment was carried out at the Seed Analysis and Image Analysis Laboratories of the Crop Production Department (LPV) of the *Escola Superior de Agricultura Luiz de Queiroz (ESALQ)*, *Universidade de São Paulo (USP)*, in Piracicaba, SP, using six lots of rice seeds of the cultivar BRS Catiana.

X-ray images

Four replications of 50 seeds of each lot were used. The seeds were fixed with double-sided adhesive tape in transparent Petri dishes with 9.0 cm diameter, positioned one by one, in a single layer and equidistant from each other, under identification sequence for subsequent tests (Figure 1.1). Radiographic images were obtained using the MultiFocus Digital Radiography System - MDRS (Faxitron Bioptics, LLC, Tucson, USA), connected to a computer (Figure 1.2). The radiographic images were saved in the specific folder of the computer's hard drive.

Then, the seeds were individually analyzed from the radiographic images and separated according to the occurrence or not of damage (mechanical damage and insect damage); seeds in which these types of damage were detected were removed from the subsequent analysis to eliminate their effects and allow the evaluation of the relationship between the internal free space of the seeds and their physiological potential. Due to the low number of seeds with these types of damage, this factor was disregarded in the statistical analyses.

To obtain the area of the internal free space of the seeds, the radiographic images were analyzed using ImageJ software, version 1.48v (Schneider et al., 2012), following the methodology proposed by Silva et al. (2012), using the *fraction area* command, which determines the internal free space of the seeds, through the separation and counting of pixels by the intensity of the color, of all seeds, individually, being expressed as a percentage. The values of total area (mm²) of the individual seeds and the relative density (gray.pixel⁻¹), representing the average pixel intensity in grayscale, were also obtained.

Acquisition of multispectral and chlorophyll fluorescence images with VideometerLab instrument

After the X-ray test, each Petri dish containing the same seeds was positioned under the integrating sphere of the VideometerLab 4 instrument (Videometer A/S, Hørsholm, Denmark) (Figure 1.3) and, after successive activation of the 19 contiguous LEDs, arranged on the rim of the sphere, the standard chip of monochrome charge-coupled device (CCD) recorded and captured seed reflectance, generating 19 spectral images corresponding to each wavelength (365, 405, 430, 450, 470, 490, 515, 540, 570, 590, 630, 645, 660, 690, 780, 850, 880, 940 and 970 nm) per sample, with resolution of 2056 x 2056 pixels.

To measure the chlorophyll fluorescence (CF) of the seeds, three filters of short optical density were added, which allowed capturing the radiation intensity of only the 700 nm wavelength (emission energy), allowing the equipment to generate three specific images of the bands corresponding to the fluorescence for the excitation energies of: 1) 630 nm (red region); 2) 645 nm (chlorophyll 'a'); 3) 660 nm (chlorophyll 'b').

Subsequently, the images obtained were processed using VideometerLab4[®] software version 3.14.9. The 'Blue background' segmentation mask was used for segmenting the background (Petri dish and noise) and the region of interest (seeds). Then, the seeds were selected individually by means of the 'full' command, which provided the average reflectance of all images of each seed; with this, the CF and the other reflectances of the bands of the corresponding spectrum were obtained.

To obtain color and texture parameters of the seeds, the supervised method nCDA (Normalized Canonical Discriminant Analysis) was used to transform the multispectral images (MSI) and segment them into regions of interest, in order to minimize or maximize the distance of observations within and between seed samples (Olesen et al., 2011). The 'blob' (Binary Large Object) command was used to analyze the seeds individually and obtain the color appearance attributes CIELab a* (green to red), CIELab b* (blue to yellow) and CIELab L (glume lightness). All data extracted from the multispectral images were exported to Excel.

Acquisition of chlorophyll 'a' fluorescence images with SeedReporter[®] instrument

To obtain chlorophyll fluorescence (CF) images, the seeds subjected to the two previously described evaluations were transferred one by one to a black and opaque polyethylene sheet under the identification sequence. Then, the sheets were placed inside the integration compartment of the instrument and the images were generated by means of the fast repetition rate fluorometry (FRRF) and the duration of the impulses. Saturating sub-pulses that excite chlorophyll 'a' were captured by a CCD (Charge-Coupled Device) camera. Excitation of chlorophyll in the seeds was induced by the emission of radiation with a wavelength of 620 nm, and the chlorophyll fluorescence signals were detected at 730 nm, using a filter with this optical density. The images were generated in the grayscale, with 320 x 240 pixels, synchronously within four-second intervals (Figure 1.4).

The images were processed with Data Analysis PhenoVation software (version 5.5.1). Each image was treated with filters for noise removal and a last filter to allow the reading of the individual CF of each seed, thus generating CF data of individual and sequenced seeds. Chlorophyll and anthocyanin indices were also obtained from the images.

Computerized analysis of seedling images (SVIS[®])

In order to evaluate the physiological performance of the seeds, computerized analysis of seedlings was performed

with SVIS® software. The seeds of each replication of each lot, from the three evaluations described above, were divided into two groups of 20 and one of 10 and placed to germinate, numbered in two rows located in the upper third of the paper towel, at 25 °C, for five days. The substrate was moistened with a volume of water equivalent to 2.5 times its mass.

The seedlings were transferred to a black cardboard sheet in order to provide the contrast needed for analysis by the system. Then, the seedling images were scanned using an HP Scanjet 200 scanner, adjusted at a resolution of 100 dpi, installed upside down inside an aluminum box (60.0 x 50.0 x 12.0 cm) connected to a computer (Figure 1.5).

The images were analyzed with the Seed Vigor Imaging System (SVIS®), generating individual seedling lengths (cm), as described by Hoffmaster et al. (2003) and Marcos-Filho et al. (2006).

Physiological tests

Next, the seeds from these lots were evaluated for physiological potential with the tests described below.

Germination: evaluated with four replications of 50 seeds in rolls of paper towel moistened with a volume of water equivalent to 2.5 times the dry paper mass, at 25 °C. The first and second counts were performed at five and 14 days, respectively, after the beginning of the test, determining the percentage of normal seedlings (Brasil, 2009).

Accelerated aging: four replications of 50 seeds were distributed in a single layer on a metal screen suspended inside transparent plastic boxes (11.0 x 11.0 x 3.0 cm), containing 40 mL of distilled water. The boxes were kept at 41 °C for 96 hours (AOSA, 2009). After this period, the germination test was set up, according to the previous item. The evaluation was performed five days after setting up the test, and the results were expressed in percentage of normal seedlings.

Seedling emergence in sand: four replications of 50 seeds were sown at 1 cm depth in plastic boxes (32.0 x 28.0 x 10.0 cm), and irrigation was applied so that the substrate reached 60% of its water holding capacity. The evaluations were performed daily, computing the number of seedlings emerged until the fourteenth day after setting up the test, determining the average percentage of seedling emergence for each lot and the seedling emergence speed index, using the method proposed by Maguire (1962).

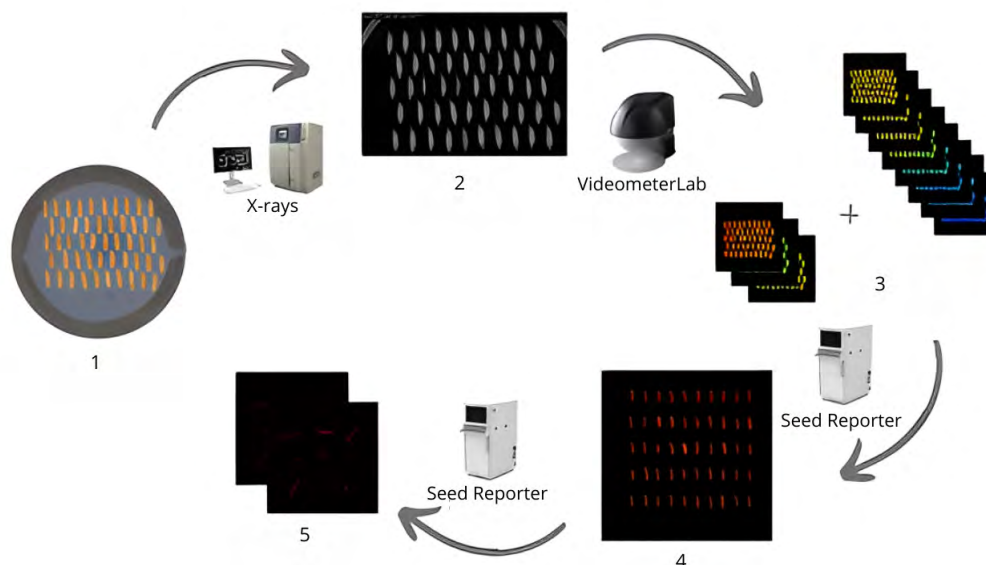


Figure 1. Flowchart of the analyses performed: positioning of the seeds of each replication in Petri dishes (1); acquisition of X-ray images (2) and multispectral and chlorophyll fluorescence images with VideometerLab instrument (3); acquisition of chlorophyll 'a' fluorescence images with the SeedReporter® instrument (4); computerized analysis of seedling images (SVIS®) (5).

Electrical conductivity: determined from the mass system according to the methodology proposed by the Seed Vigor Committee of AOSA (2009). Four replications of 50 seeds were previously weighed on a precision scale (0.001 g); then, the seeds were placed in plastic cups filled with 75 mL of distilled water. The cups were kept for 24 hours at 25 °C (Custódio and Marcos-Filho, 1997). At the end of this procedure, the electrical conductivity of the solution was measured using the DIGIMED® device, model DM-32. The results were expressed in $\mu\text{S}\cdot\text{cm}^{-1}\cdot\text{g}^{-1}$ of seeds.

Computerized analysis of seedling images (SVIS®): five replications of 20 seeds per lot were used, following the methodology described above. The images were analyzed by the Seed Vigor Imaging System (SVIS®) software, and the development uniformity and vigor indices were generated according to Sako et al. (2001), comprising values from 0 to 1000; seed vigor is directly proportional to these values. After processing the images, the mean values of vigor and development uniformity indices and length of seedlings (cm) were obtained for each lot, as described by Hoffmaster et al. (2003) and Marcos-Filho et al. (2006).

In order to monitor the moisture content of the seeds during the previous tests, their water content was determined by the method of oven at 105 (± 3 °C) for 24 hours (Brasil, 2009), with two replications of 5 g of seeds for each lot. The results were expressed in percentage (wet basis). This determination was also carried out after the accelerated aging test.

Statistical analysis

The results obtained in the germination, vigor and image parameters tests were subjected to analysis of variance, in a completely randomized experimental design, and the means of the lots were grouped by the Scott-Knott test ($p \leq 0.05$). Multivariate analysis, including principal component analysis (PCA) and Pearson's correlation coefficients (r), were performed for all image parameters obtained and for germination and vigor data. Based on the germination test, the seeds that underwent image analysis were classified into two groups: germinated and not germinated, or originating abnormal seedlings. Then, the classes were subjected to analysis of variance, for the variables free space, spectral bands, and CF of 630/700 nm, 645/700 nm, 660/700 nm and 620/730 nm, in a completely randomized experimental design, and the means were grouped by the Scott-Knott test ($p \leq 0.05$). The statistical analysis were performed using R software (R Core Team, 2018).

RESULTS AND DISCUSSION

According to Figure 2A, seeds of lots 1 and 2 showed higher mean values of free space, with 9.18% and 7.85%, respectively, whereas the other lots did not differ statistically from one another. Uniformity was verified in the area of the seeds of the evaluated lots (Figure 2B), without statistically significant differences, which indicates that, for the tested lots, this parameter is not affected by possible differences in the internal content of the seeds. The analysis of radiographic images based on estimates of relative density using ImageJ software was not able to discriminate the seed lots (Figure 2C).

Chlorophyll 'a' fluorescence analysis with the *SeedReporter*® of 620/730 nm (excitation/emission energy) allowed the separation of seed lots (Figure 5D), with the highest average intensity for lot 3 (5537.11) and the lowest average intensity for lot 4 (3931.03). Figure 2E shows that the values of chlorophyll content of the seeds, measured by the chlorophyll index, were higher for lots 2 and 5, intermediate for lots 1 and 6 and lower for lots 3 and 4.

The anthocyanin index showed the lower value for lot 3, intermediate value for lot 1 and higher values for the other lots, which showed a similar behavior compared to each other (Figure 2F).

The mean reflectance spectra at the wavelengths of the 19 spectral bands, obtained by the VideometerLab instrument, showed statistical differences between the seed lots (Figure 3), with higher average intensity for lot 3. It is worth pointing out that the spectral behavior of the seeds varied according to the spectral band, for instance the

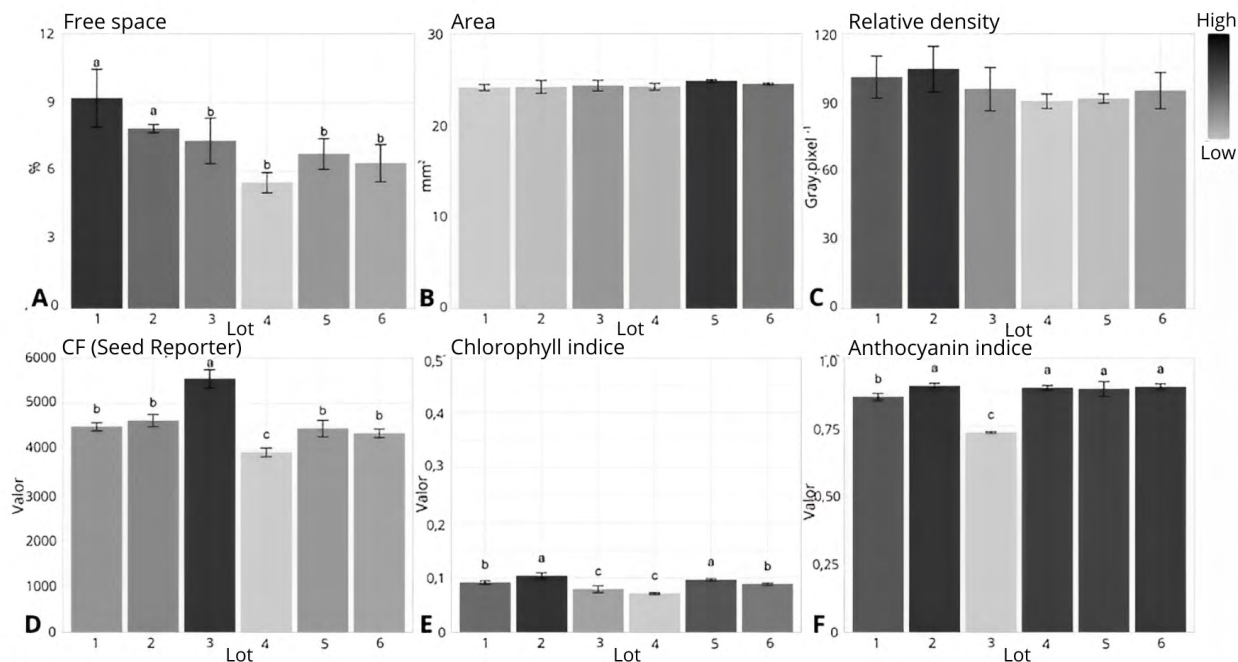


Figure 2. Variables obtained with X-ray image analysis: free space (A), seed area (B) and relative density (C); with chlorophyll fluorescence images of 620/730 nm – excitation/emission energy: chlorophyll fluorescence (D), chlorophyll index (E) and anthocyanin index (F), of seeds from six lots of the rice cultivar BRS Catiana. Different letters above each column, for each evaluation, indicate that the lots belong to different groups by the Scott-Knott test ($p < 0.05$). Bars represent the standard deviation.

wavelength of 470 nm (Band 5). Only lot 3 differed from the others, with higher mean value, whereas at wavelengths of 630, 645, 660 and 690 nm (Bands 11, 12, 13 and 14) there was greater discrimination between the lots.

The chlorophyll fluorescence measured by the VideometerLab instrument (Figure 3), corresponding to the bands of 630/700 nm (red region), 645/700 nm (chlorophyll 'a'), 660/700 nm (chlorophyll 'b'), excitation/emission energies (Bands 21, 22 and 23), showed spectral behaviors similar to that of chlorophyll 'a' fluorescence measured with the *SeedReporter*[®] instrument, with significant positive correlation (Figure 8), and higher values were observed for lot 3, with 50.170 (630/700 nm), 100.754 (645/700 nm) and 91.325 (660/700 nm).

Based on the nCDA (Normalized Canonical Discriminant Analysis) model of VideometerLab, the color parameters showed means with different behaviors for the seed lots. According to Figure 3, the CIELab L attribute showed a similar pattern of means for the 19 spectral bands, with the highest mean for lot 3 (67.49) and the lowest means for lots 1 and 2 (63.49 and 64.04, respectively). For the attributes CIELab a* and CIELab b*, lot 3 showed the lowest means (8.00 and 24.01, respectively).

According to the seed germination test and its results, illustrated in Figure 4A, seeds of lot 2 had the highest mean (96%), followed by seeds of lots 3, 5 and 4 (94%, 92% and 91%, respectively) with intermediate means and, finally, seeds of lots 6 and 1 (89% and 85%, respectively) with the lowest means.

In relation to vigor tests, the first germination count test showed the highest value for lot 2, followed by lots 5 and 6 (with lot 5 having higher value than lot 6), and with the lowest values for the other lots, which showed similar performance compared to each other (Figure 4B).

Regarding the results of the accelerated aging test (Figure 4C) and seedling emergence in sand (Figure 4E), seeds of lots 2 and 5 showed higher percentages compared to the other lots, which did not differ from each other.

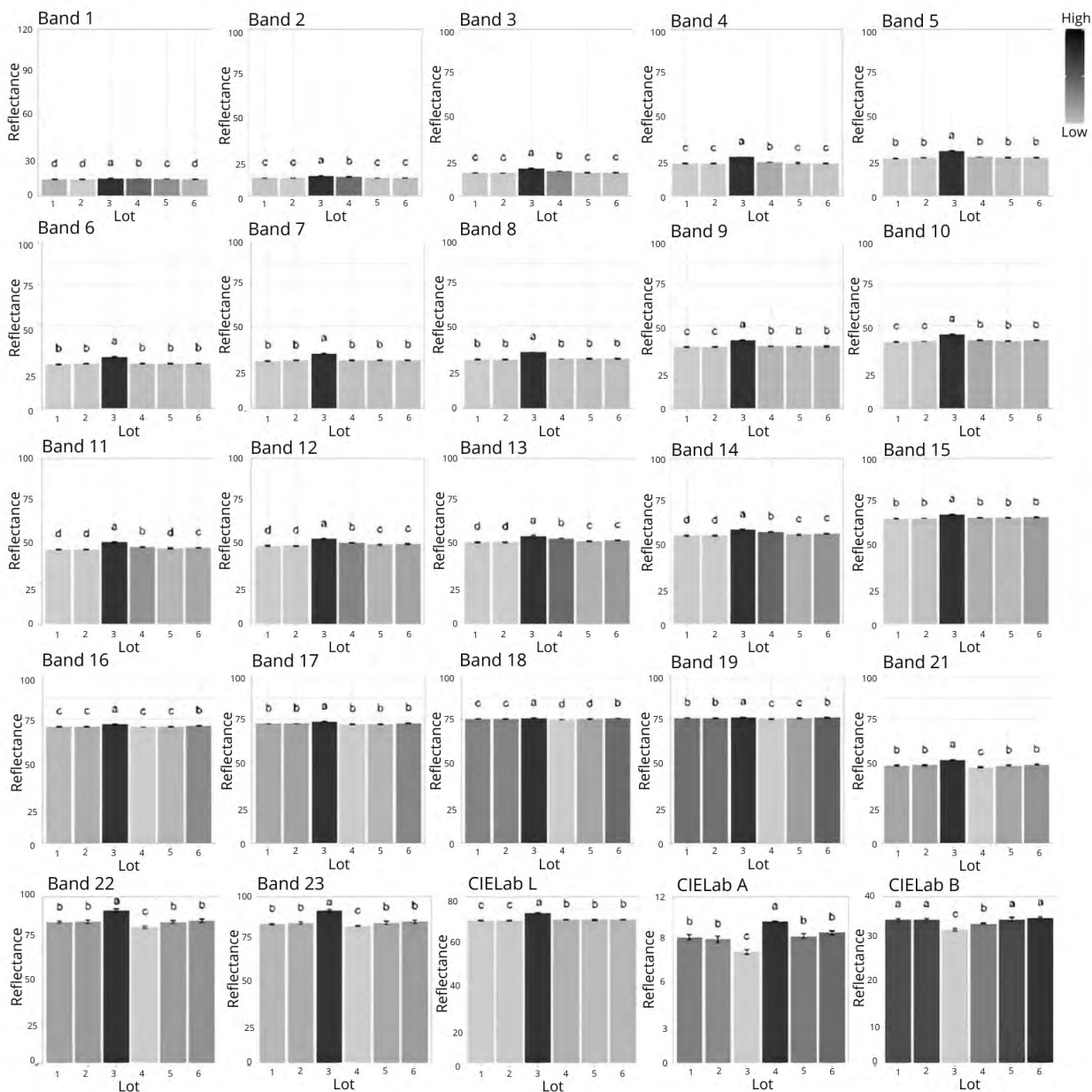


Figure 3. Multispectral analyses, corresponding to 22 spectral bands (365, 405, 430, 450, 470, 490, 515, 540, 570, 590, 630, 645, 660, 690, 780, 850, 880, 940, 970, 630/700, 645/700, 660/700 nm, respectively) with individual and color charts (CIELab L, CIELab a* and CIELab b*) of six lots of BRS Catiana rice seeds. Different letters above the columns, for each evaluation, indicate that the lots belong to different groups by the Scott-Knott test ($p < 0.05$). Bars represent the standard deviation.

For electrical conductivity (Figure 4D), lots 3 and 1 had the highest values, followed by lots 5, 6 and 2, which showed intermediate values, and lot 4 had the lowest value.

It was observed in the evaluation with SVIS software that lot 2 had the highest total length of seedlings, followed by lot 3, lot 6 and lot 4, respectively, with lot 1 showing the shortest length compared to the others (Figure 4F). Regarding the vigor index (Figure 4G), higher values were found for lots 2 and 6, while the other lots showed similar values. For the development uniformity index, there was no difference in performance among the lots (Figure 4H).

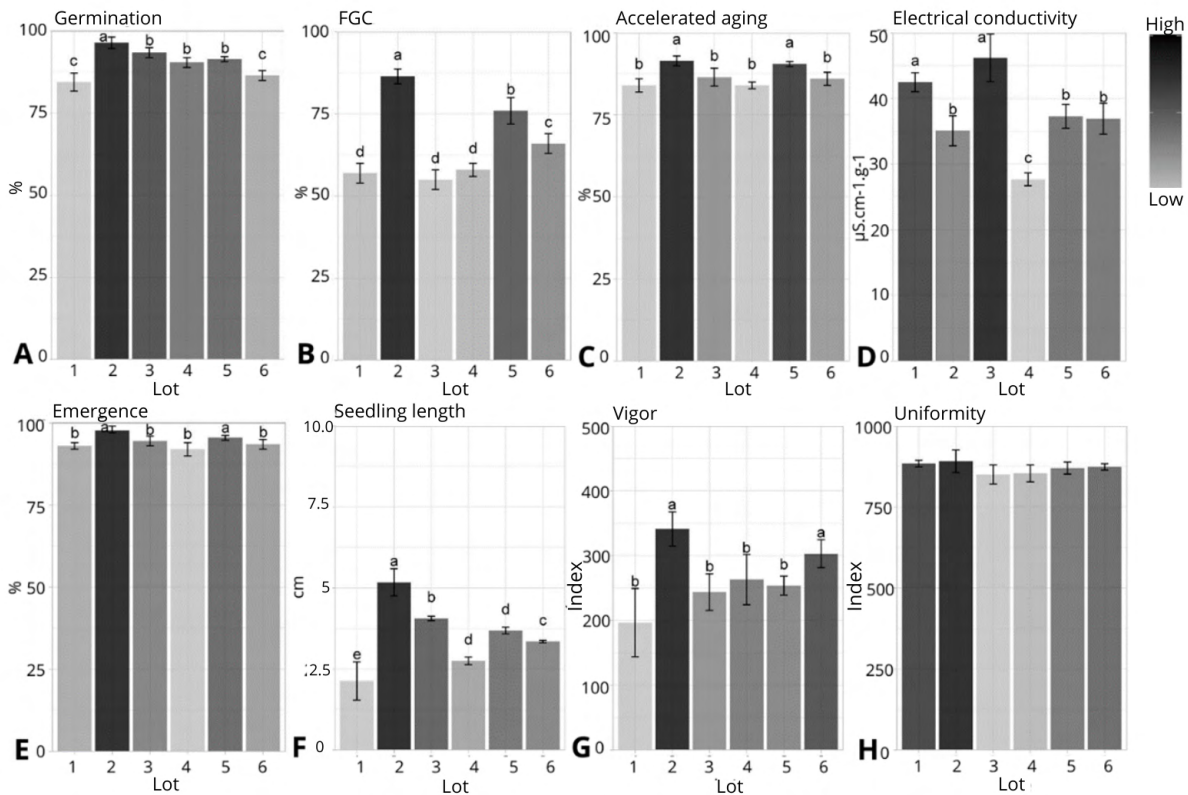


Figure 4. Germination (A), first germination count (B), accelerated aging (C), electrical conductivity (D), seedling emergence in sand (E), seedling length (F), vigor index (G), development uniformity index (H) of seeds from six lots of the rice cultivar BRS Catiana. Different letters above the columns, for each evaluation, indicate that the lots belong to different groups by the Scott-Knott test ($p < 0.05$). Bars represent the standard deviation.

The data obtained in the analysis of radiographic, multispectral and CF images of the seeds were subjected to principal component analysis (PCA) (Figure 5A). The first two principal components explained 79.5% of the total variance between imaging parameters and the physiological potential of individual seed lots, with 59.2% and 20.3% for PC1 and PC2, respectively. There was separation of rice seed lots, with lot 3 having higher values of spectral band reflectance and color and CF characteristics, while lot 4 had lower values in vigor and germination tests, with lower values of spectral band reflectance and color and CF characteristics.

In general, for the parameters obtained in the analysis of X-ray images (free space, seed area and relative density), considering the mean values of the lots, no significant correlations were found with germination and vigor tests with none of the parameters of multispectral and CF images of the seed lots (Figure 5B).

The area occupied by the embryo and endosperm inside the seeds, in average values, was not related to the physiological potential of the seeds (Figure 5B). In fact, lots that had seeds with higher percentage of free space (lots 1 and 2) showed different physiological performances, with lower values in germination and vigor tests for lot 1 and higher values for lot 2. Again, it is important to highlight that the fact that higher mean values of free spaces were observed in seeds of lots 1 and 2 does not mean that their germination and vigor were compromised. Gomes-Junior (2010) observed that castor bean seeds with larger embryonic area do not necessarily generate seedlings with greater length and the relationship between seed internal morphology and physiological potential is not always verified, as also observed in eggplant (Silva et al., 2012) and bell pepper (Gagliardi and Marcos-Filho, 2011).

The relative density of the seed refers to the levels of radioluminescence (dark) and radiopacity (light) of the radiographic image in grayscale and may be indirectly related to tissue deterioration, mechanical damage and filling of the embryo and endosperm inside the seeds (Medeiros et al., 2018). In rice seeds, with the lots under study, this parameter showed no correlation with the physiological potential (Figure 5B). Similar results were also observed in mung bean (*Vigna radiata* L.) seeds by Machado et al. (2020), who found that the relative density depends on characteristics of the seed of the studied species, such as oil and carbohydrate contents, thickness, among others.

According to the analysis presented in Figure 5B, the mean electrical conductivity of the seed lots was the only physiological parameter that showed significant correlation with multispectral data, in the spectral bands of 940 nm and 970 nm (Bands 18 and 19). This variable also showed correlation with the chlorophyll 'a' fluorescence band at excitation/emission energy of 645/700 nm (Band 22) and chlorophyll 'a' fluorescence with the *SeedReporter*[®] instrument, of excitation/emission energy of 620/730 nm. The electrical charge of the chlorophyll molecule directly

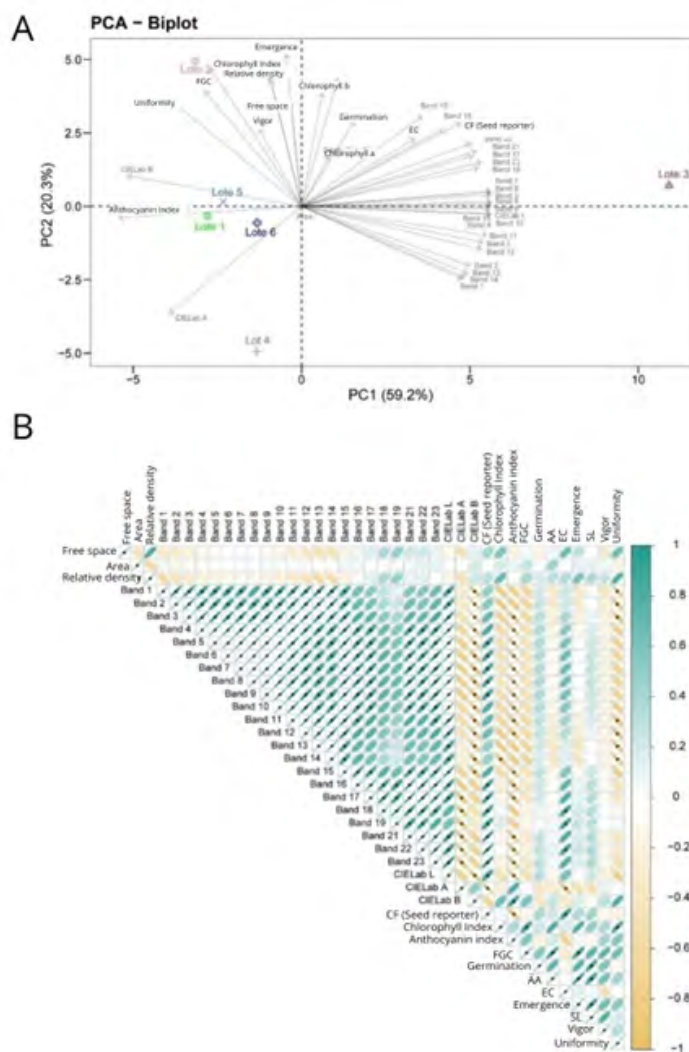


Figure 5. A: Biplot of principal component analysis obtained from the variables related to X-ray, multispectral, chlorophyll fluorescence and physiological analyses of seeds of the rice cultivar BRS Catiana. PC1 - Principal Component 1; PC2 - Principal Component 2. B: Estimates of Pearson's correlations between the multiple characteristics of X-ray, multispectral, chlorophyll fluorescence and physiological analyses of six lots under study. FGC - first germination count; AA - accelerated aging; EC - electrical conductivity; Emergence - seedling emergence in sand; SL - seedling length; Uniformity - development uniformity index; Vigor - vigor index.

affects the electrical conductivity of the soaking solution, as this molecule is very sensitive to chemical degradation, so electrons are released into the aqueous solution (Porra et al., 1989). Thus, for seeds with higher CF intensity, there is greater interference of the amount of electrolytes released by chlorophyll.

The finding that the mean CF data of the seeds of the six lots were not significantly correlated with the data of germination and vigor tests, except for electrical conductivity (Figure 5B), may indicate that, considering mean values of the lots, the individualities of the seeds are not being taken into account. Thus, the lots may have similar mean CF values, but with seeds showing different germination and vigor values, i.e., some seeds may have higher CF values and other seeds may have lower values, with different effects on germination and vigor. Figure 6 exemplifies these individualities: seeds 1, 2 and 3, from different lots with similar mean CF values, showed chlorophyll 'a' fluorescence (620/730 nm) values of 3865 (Figure 6.1a), 3576 (Figure 6.2a) and 3694 (Figure 6.3a), as well as chlorophyll 'a' fluorescence (645/700 nm) means of 91.19 (Figure 6.1b), 85.58 (Figure 6.2b) and 87.66 (Figure 6.3b), and chlorophyll 'b' fluorescence (660/700 nm) means of 85.30 (Figure 6.1c), 80.54 (Figure 6.2c) and 81.13 (Figure 6.3c). However, when the seeds were subjected to the germination test, they exhibited different behaviors, with seed 1 originating a dead seed (Figure 6.1d) and with seeds 2 and 3 originating, respectively, seedlings with total length of 0.78 cm and 2.61 cm at five days after sowing (Figures 6.2d and 6.3d), indicating differences in seed viability and vigor.

Considering all seeds of all lots, the means of reflectance of those that were subjected to germination test and generated dead seeds or originated abnormal seedlings and those that generated normal seedlings differed statistically in the spectral bands with wavelength from 590 nm to 780 nm and in the band of 970 nm (Figure 7).

It can be seen in Figure 8 that seeds that did not germinate or originated abnormal seedlings showed higher mean value of chlorophyll fluorescence of the red region – 630/700 nm (A) and chlorophyll 'a' region – 645/700 nm (B), with significant statistical difference between them, while the means of chlorophyll 'b' fluorescence, 660/700 nm (C), and

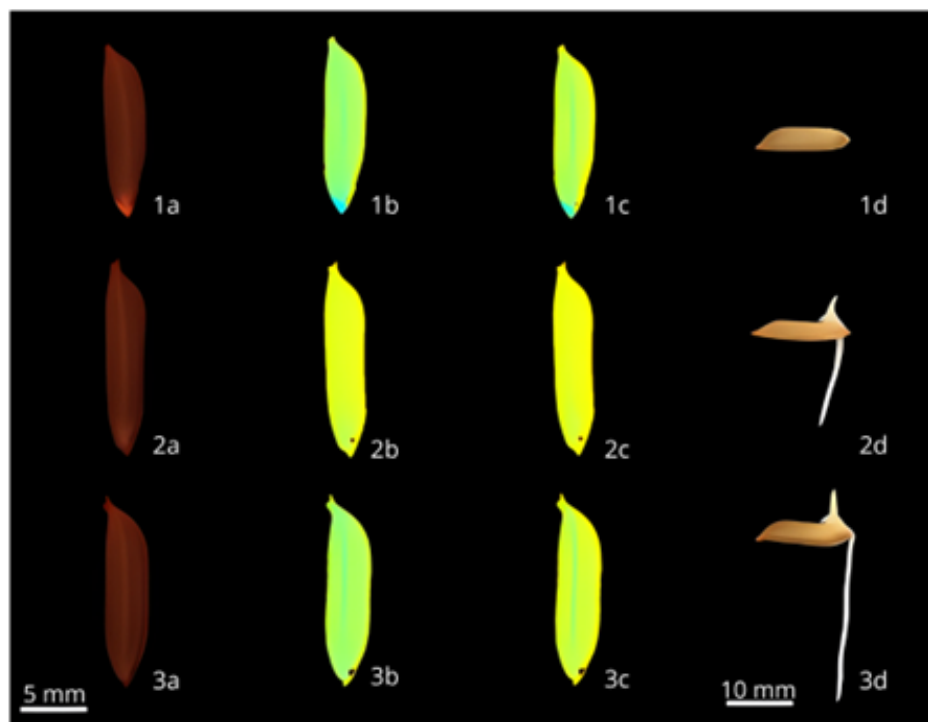


Figure 6. Images of seeds of the rice cultivar BRS Catiana with similar mean values of chlorophyll 'a' fluorescence at 620/730 nm (1a, 2a and 3a), chlorophyll 'a' fluorescence at 645/700 nm (1b, 2b and 3b) and chlorophyll 'b' fluorescence at 660/700 nm (1c, 2c and 3c), originating dead seed (1d) and seedlings with different lengths (2d and 3d).

chlorophyll 'a' fluorescence, 620/730 nm (D), showed no statistically significant difference between them. Similar results were also observed by Jalink et al. (1998), who found that the magnitude of chlorophyll fluorescence in cabbage (*Brassica oleracea* L.) seeds is inversely related to germination performance or the capacity to generate normal seedlings. Jalink et al. (1998; 1999) observed that the germination of cabbage seeds was higher in those with low CF signal. Similar results were also observed by Cicero et al. (2009), in soybean seeds, and by Xing et al. (2010), in wheat seeds.

Also in Figure 8, it is possible to observe that seeds that had chlorophyll fluorescence values at 630/700 nm and 645/700 nm equal to or higher than 55.58 and 112.92, respectively, did not germinate or originated abnormal seedlings.

The average percentage of free space in the internal cavity of rice seeds that did not germinate or originated abnormal seedlings (14.68%) was higher than that found in seeds that generated normal seedlings (6.96%), with significant statistical difference (Figure 8). It is worth pointing out that seeds that obtained free space values equal to or greater than 18.68% did not germinate or originated abnormal seedlings.

Other studies showed similar results for seeds of other species, as in 'aroeira branca' (*Lithraea molleoides*) seeds, whose germination was related to the space occupied by the embryo in the embryonic cavity (Machado and Cicero, 2003), low germination of castor bean seeds with the internal cavity filling below 50% (Carvalho et al., 2010), and the large area of the free space of the internal cavity of bell pepper seeds, which generated increase in the percentage of abnormal seedlings or non-germinated seeds (Gagliardi and Marcos-Filho, 2011).

Dell'Aquila (2007) observed that the area occupied by the embryo + endosperm in bell pepper seeds, when less than 97%, compromised germination due to the increase in the number of abnormal seedlings. Embryo development is directly linked to the success in the germination process; in addition, the greater amount of reserve tissues, due to the larger area occupied by the endosperm, represents greater availability of reserves to be assimilated during germination (Liu et al., 2005). In Figure 9, it is possible to observe a seed (Seed 1) with low percentage of free space in the internal

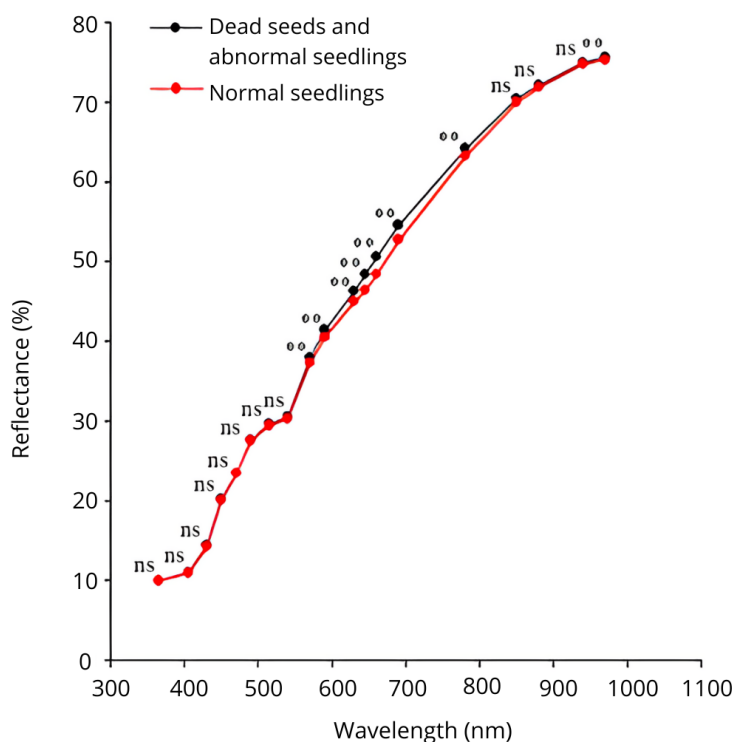


Figure 7. Mean spectral intensity of 19 wavelengths (nm) for seeds that did not germinate or originated abnormal seedlings and seeds that generated normal seedlings of the rice cultivar BRS Catiana. ** indicates significant difference between non-germinated and germinated seeds by the Scott-Knott test ($p < 0.05$).

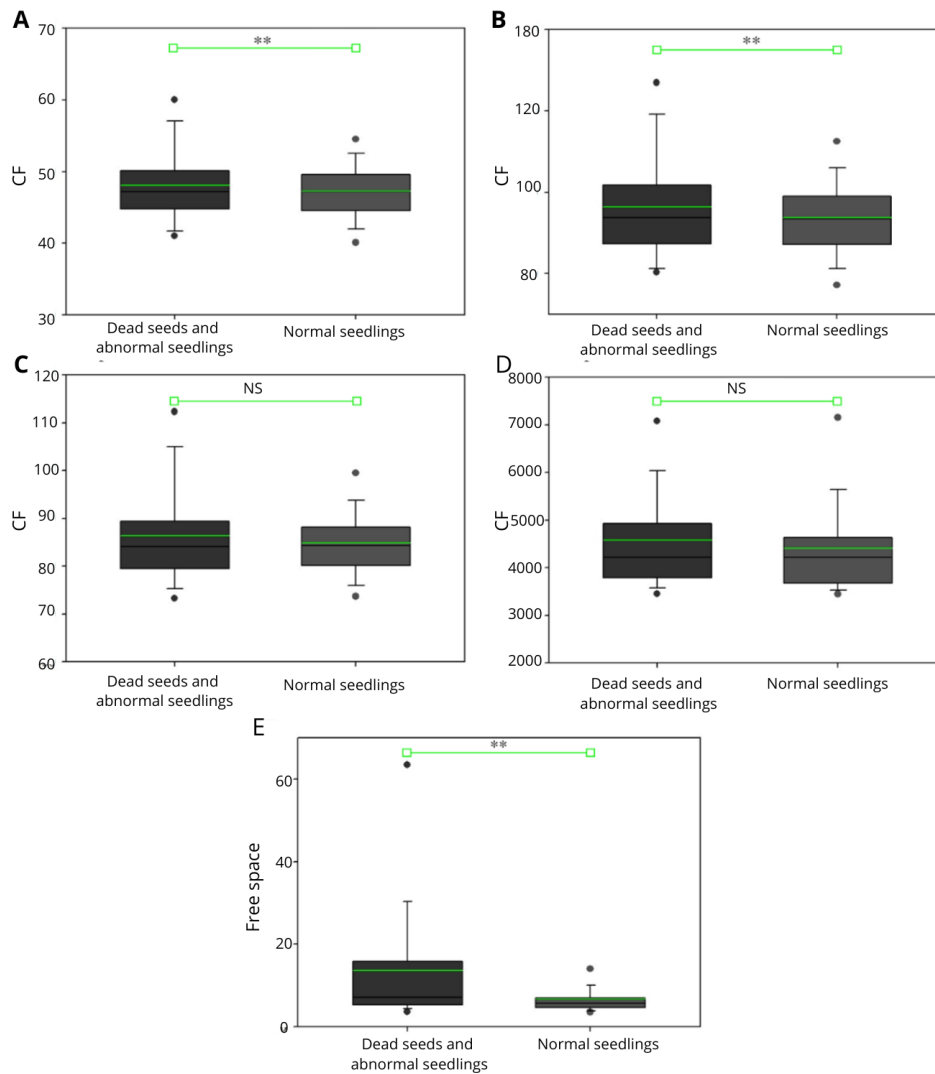


Figure 8. Differences between seeds that did not germinate or originated abnormal seedlings and seeds that generated normal seedlings of the rice cultivar BRS Catiana, in chlorophyll fluorescence of the red region - 630/700 nm (A), chlorophyll 'a' fluorescence - 620/730 nm (D) and percentage of free space in the internal cavity (E). ** indicates a significant difference between seeds not germinated and germinated by the F test ($p < 0.05$). NS indicates that there is no significant difference. Green line represents the mean. The bars represent the standard deviation.

cavity (4.56%), having a large area occupied by the endosperm and embryo tissues (Figure 9A), besides having low mean values of chlorophyll 'a' fluorescence at 620/730 nm (4380), chlorophyll 'a' fluorescence at 645/700 nm (88.76) and chlorophyll 'b' fluorescence (87.64), represented in Figures 9B, 9C and 9D, respectively. This seed showed a reflectance pattern of 19 spectral bands (Figure 9E), following low values in the red and NIR wavelengths, with a spectral pattern of seeds that generated normal seedlings (Figure 7), as the seed in question, resulting in a normal seedling with 2.97 cm in total length at 11 days after emergence (Figure 9F).

On the other hand, also in Figure 9, it is possible to see a seed (Seed 2) with a high percentage of free space in the internal cavity (19.68%), with compromised embryonic and endospermic development (Figure 9A); in addition, the mean values of CF were high: chlorophyll 'a' fluorescence at 620/730 nm (69.13), chlorophyll 'a' fluorescence at

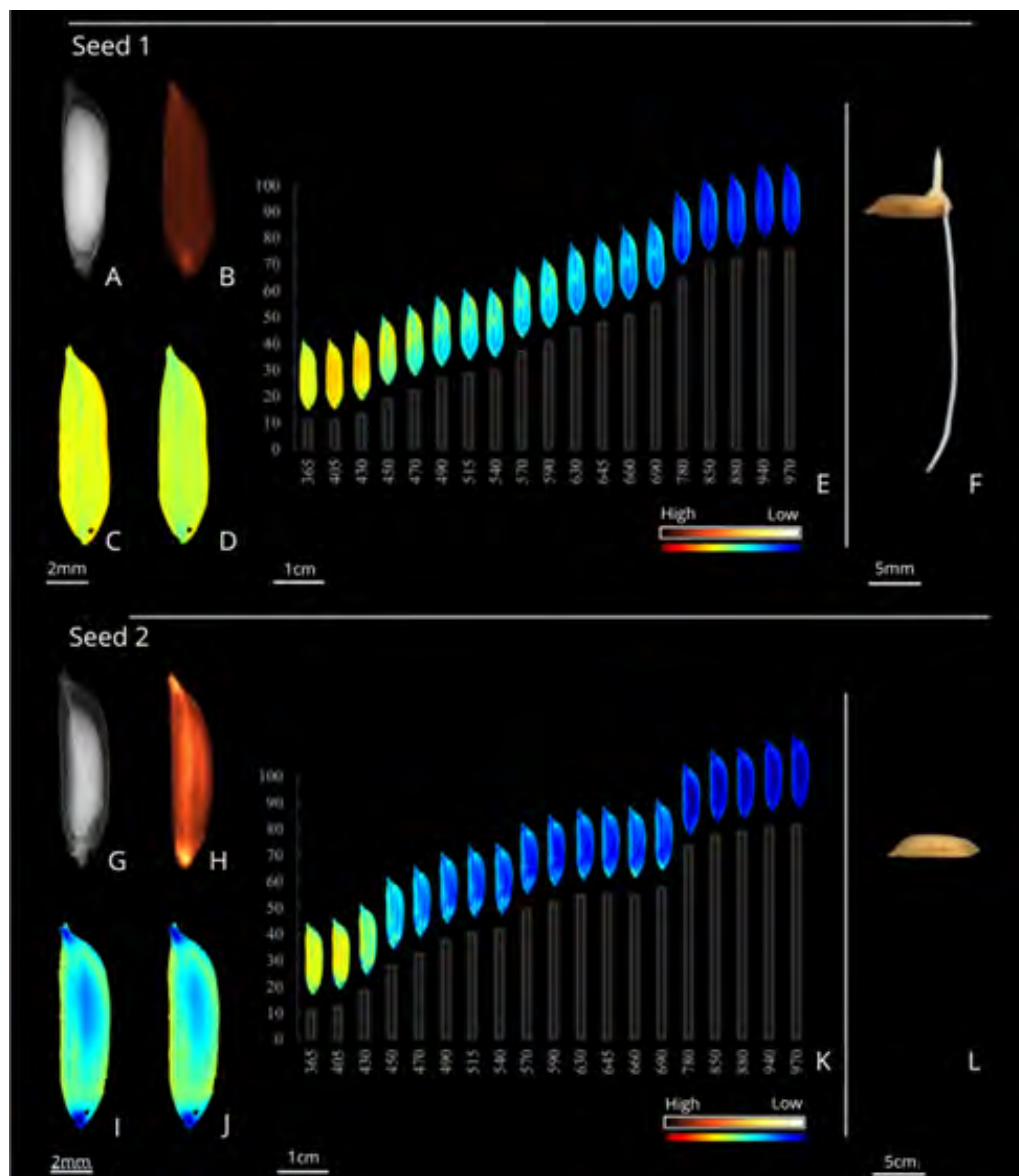


Figure 9. Images of seeds of the rice cultivar BRS Catiana: seed 1 - with low percentage of free space in the internal cavity, measured from radiographic image (A) and low mean values of chlorophyll 'a' fluorescence at 620/730 nm (B), chlorophyll 'a' fluorescence at 645/700 nm (C) and chlorophyll 'b' fluorescence at 660/700 nm (D), and 19 spectral bands using the 'Inverse jet' filter (VideometerLab4® software), with the respective histogram of reflectance (E), originating a normal seedling (F); seed 2 - with high percentage of free space in the internal cavity, measured from radiographic image (G) and high mean values of chlorophyll 'a' fluorescence at 620/730 nm (H), chlorophyll 'a' fluorescence at 645/700 nm (I) and chlorophyll 'b' fluorescence at 660/700 nm (J), and 19 spectral bands using the 'Inverse jet' filter (VideometerLab4® software), with the respective histogram of reflectance (K), originating a dead seed (L).

645/700 nm (152.22) and chlorophyll 'b' fluorescence at 660/700 nm (135.39), represented in Figures 9B, 9C and 9D, respectively. The reflectance pattern of 19 spectral bands of the seed (Figure 9E) showed higher values in the red and NIR wavelengths, when compared to the seed presented in Figure 7, which followed a spectral pattern of seeds that generated normal seedlings, and in turn, the seed presented in Figure 9F showed a spectral pattern of seeds that did not germinate (Figure 7).

Thus, it is verified that X-ray, multispectral and chlorophyll fluorescence images are important techniques for non-destructive and reliable analysis of rice seed quality. The degree of embryonic development, from the free space in the internal cavity of the rice seed, is directly associated with its performance, with the possibility of use in the seed industry. On the other hand, the techniques of multispectral and chlorophyll fluorescence images constitute a technology that associates computer vision and spectroscopy to obtain spatial and spectral information of rice seeds, without the need for pre-treatments, which can open new possibilities for real-time monitoring of seeds with the integration of optical sensors. However, to increase the reliability and reproducibility of these techniques, the integration of properly calibrated systems is essential to avoid saturation and incorrect measurements. In addition, the cost and lifespan of the instruments (hardware and software) should be considered to construct a viable, on-line optical imaging system, i.e., with real-time monitoring of the process.

CONCLUSIONS

Rice seeds with internal free space equal to or greater than 18.68% do not germinate or originate abnormal seedlings.

Rice seeds that do not germinate or originate abnormal seedlings show greater reflectance in spectral bands with wavelengths from 590 nm to 780 nm (41.46% to 64.21%, respectively) and in the band of 970 nm (75.65%).

Immature rice seeds that do not germinate or originate abnormal seedlings and show chlorophyll fluorescence values equal to or higher than 55.58 and 112.92 at excitation/emission energies of 630/700 nm and 645/700 nm, respectively.

ACKNOWLEDGMENTS

To the National Council for Scientific and Technological Development (CNPq), for granting a scholarship to the first author. To the São Paulo State Research Support Foundation - FAPESP, for enabling the use of VideometerLab, SeedReporter and MultiFocus Radiography System, associated with the *Jovem Pesquisador em Centros Emergentes* project - Process 2017/15220-7.

REFERENCES

- AOSA. Association of Official Seed Analysts. *Seed vigor testing handbook*. Springfield: AOSA, 2009. 341p.
- BRASIL. Ministério da Agricultura, Pecuária e Abastecimento. *Regras para Análise de Sementes*. Ministério da Agricultura, Pecuária e Abastecimento. Secretaria de Defesa Agropecuária. Brasília: MAPA/ACS, 2009. 399p. https://www.gov.br/agricultura/pt-br/assuntos/insumos-agropecuarios/arquivos-publicacoes-insumos/2946_regras_analise__sementes.pdf
- CARVALHO, M.L.M.; ALVES, R.A.; OLIVEIRA, L.M. Radiographic analysis in castor bean seeds (*Ricinus communis* L.). *Revista Brasileira de Sementes*, v.32, n.1, p.170-175, 2010. <https://doi.org/10.1590/S0101-31222010000100019>
- CICERO, S.M.; VAN DER SCHOOR, R.; JALINK, H. Use of chlorophyll fluorescence sorting to improve soybean seed quality. *Revista Brasileira de Sementes*, v.31, n.4, p.145-151, 2009. <https://doi.org/10.1590/S0101-31222009000400017>
- CUSTÓDIO, C.C.; MARCOS-FILHO, J. Potassium leachate test for the evaluation of soybean seed physiological quality. *Seed Science and Technology*, v.25, n.3, p.549-564, 1997.
- DELL'AQUILA, A. Pepper seed germination assessed by combined X radiography and computer-aided imaging analysis. *Biologia Plantarum*, v.51, n.4, p.777-781, 2007. <http://dx.doi.org/10.1007/s10535-007-0159-9>
- GAGLIARDI, B.; MARCOS-FILHO, J. Relationship between germination and bell pepper seed structure assessed by the X-ray test. *Scientia Agricola*, v.68, n.4, p.411-416, 2011. <https://doi.org/10.1590/S0103-90162011000400004>
- GOMES-JUNIOR, F.G. Aplicação da análise de imagens para avaliação da morfologia interna de sementes. *Informativo Abrates*, v.20, n.3, p.33-39, 2010. https://www.researchgate.net/publication/259713976_Aplicacao_da_analise_de_imagens_para_avaliacao_da_morfologia_interna_de_sementes

- HOFFMASTER, A.L.; FUJIMURA, K.; MCDONALD, M.B.; BENNETT, M.A. An automated system for vigor testing three-day old soybean seedlings. *Seed Science and Technology*, v.31, n.3, p.701-713, 2003. <http://dx.doi.org/10.15258/sst.2003.31.3.19>
- HUANG, M.; WANG, Q.G.; ZHU, Q.B.; QIN, J.W.; HUANG, G. Review of seed quality and safety tests using optical sensing technologies. *Seed Science and Technology*, v.43, p.337-366, 2015. <http://dx.doi.org/10.15258/sst.2015.43.3.16>
- JALINK, H.; FRANDAS, A.; VAN DER SCHOOR, R.; BINO, J.B. Chlorophyll fluorescence of the testa of *Brassica oleracea* seeds as an indicator of seed maturity and seed quality. *Scientia Agricola*, v.55, p.88-93, 1998. <http://dx.doi.org/10.1590/S0103-90161998000500016>
- JALINK, H.; VAN DER SCHOOR, R.; BIRNBAUM, Y.E.; BINO, R.J. Seed chlorophyll content as an indicator for seed maturity and seed quality. *Acta Horticulturae*, v.504, n.12, p.219-228, 1999. <http://dx.doi.org/10.17660/ActaHortic.1999.504.23>
- LI, C.; WANG, X.; MENG, Z. Tomato seeds maturity detection system based on chlorophyll fluorescence. *Optical Design and Testing VII*, v.10021, p.1-7, 2016. <http://dx.doi.org/10.1117/12.2247866>
- LIU, Z.H.; CHENG, F.M.; CHENG, W.D.; ZHANG, G.P. Positional variations in phytic acid and protein content within a panicle of japonica rice. *Journal of Cereal Science*, v.41, p.297-303, 2005. <http://dx.doi.org/10.1016/j.jcs.2004.09.010>
- MACHADO, C.F.; CICERO, S.M. 'Aroeira branca' seed quality evaluation by the X-ray test. *Scientia Agricola*, v.60, n.2, p.393-397, 2003. <http://dx.doi.org/10.1590/S0103-90162003000200026>
- MACHADO, T.P.M.; MEDEIROS, A.D.; PINHEIRO, D.T.; SILVA, L.J.; DIAS, D.C.F. S. Non-destructive identification of physical damage in mung bean (*Vigna radiata* L.) seeds by x-ray image analysis. *Bioscience Journal*, v.36, n.3, p.932-941, 2020. <http://dx.doi.org/10.14393/BJ-v36n3a2020-47783>
- MAGUIRE, J.D. Speed of germination-aid in selection and evaluation for seedling emergence and vigor. *Crop Science*, v.2, p.176-177, 1962. <http://dx.doi.org/10.2135/cropsci1962.0011183X000200020033x>
- MARCOS-FILHO, J.; BENNETT, M.A.; EVANS, A.S.; GRASSBAUGH, E.M. Assessment of melon seed vigour by an automated computer imaging system compared to traditional procedures. *Seed Science and Technology*, v.34, n.2, p.507-519, 2006. <http://dx.doi.org/10.15258/sst.2006.34.2.23>
- MARCOS-FILHO, J.; GOMES-JUNIOR, F.G.; BENNETT, M.A.; WELLS, A.A.; STIEVE, S. Using tomato analyzer software to determine embryo size in X-rayed seeds. *Revista Brasileira de Sementes*, v.32, n.2, p.146-153, 2010. <http://dx.doi.org/10.1590/S0101-31222010000200018>
- MEDEIROS, A.D.; ARAÚJO, J.O.; ZAVALA-LEÓN, M.J.; SILVA, L.J.; DIAS, D.C.F.S. Parameters based on x-ray images to assess the physical and physiological quality of *Leucaena leucocephala* seeds. *Ciência e Agrotecnologia*, v.42, n.6, p.643-652, 2018. <http://dx.doi.org/10.1590/1413-70542018426023318>
- OLESEN, M.H.; CARSTENSEN, J.M.; BOELT, B. Multispectral imaging as a potential tool for seed health testing of spinach (*Spinacia oleracea* L.). *Seed Science and Technology*, v.39, p.140-150, 2011. <https://doi.org/10.15258/sst.2011.39.1.12>
- OOMS, D.; DESTAIN, M.S. Evaluation of chicory seeds maturity by chlorophyll fluorescence imaging. *Biosystems Engineering*, v.110, p.168-177, 2011. <https://doi.org/10.1016/j.biosystemseng.2011.07.012>
- PORRA, R.; THOMPSON, W.A.; KRIEDEMANN, P.E. Determination of accurate extinction coefficients and simultaneous equations for assaying chlorophylls a and b extracted with for different solvents: verification of the concentration of chlorophyll standards by atomic spectroscopy. *Biochimic Biophysic Acta*, v.975, p.384-394, 1989. [https://doi.org/10.1016/S0005-2728\(89\)80347-0](https://doi.org/10.1016/S0005-2728(89)80347-0)
- R CORE TEAM. *R Development Core Team. R: a language and environment for statistical computing*. 2018. Available at: <https://www.r-project.org/>
- SAKO, Y.; MCDONALD, M.B.; FUJIMURA, K.; EVANS, A.F.; BENNETT, M.A. A system for automated seed vigour assessment. *Seed Science and Technology*, v.29, p.625-636, 2001. <https://doi.org/10.6084/M9.FIGSHARE.1226438>
- SCHNEIDER, C.A.; RASBAND, W.S.; ELICEIRI, K.W. "NIH Image to ImageJ: 25 years of image analysis". *Nature Methods*, v.9, p.671-675, 2012. <https://doi.org/10.1038/nmeth.2089>

SILVA, C.B.; LOPES, M.M.; MARCOS-FILHO, J.; VIEIRA, R.D. Automated system of seedling image analysis (SVIS) and electrical conductivity to assess sun hemp seed vigor. *Revista Brasileira de Sementes*, v.34, n.1, p.55-60, 2012. <https://doi.org/10.1590/S0101-31222012000100007>

XING, J., SYMONS, S., SHAHIN, M.; HATCHER, D. Detection of sprout damage in Canada western red spring wheat with multiple wavebands using visible/near-infrared hyperspectral imaging. *Biosystems Engineering*, v.106, p.188-194, 2010. <https://doi.org/10.1016/j.biosystemseng.2010.03.010>

YADAV, S.K.; JALINK, H.; GROOT, S.P.C.; VAN DER SCHOOR, R.; YADAV, S.; MADLANI, M.; KODDLE, J. Quality improvement of aged cabbage (*Brassica oleracea* var. capitata) seeds using chlorophyll fluorescence sensor. *Scientia Horticulturae*, v.189, p.81–85, 2015. <https://doi.org/10.1016/j.scienta.2015.03.043>

